JOURNAL OF CATALYSIS 148, 334–340 (1994)

New Insights into $VOPO_4$ Phases through Their Hydration

Farid Benabdelouahab,* Jean-Claude Volta,† and René Olier*,[1]

*Laboratoire de Physicochimie des Interfaces, URA CNRS 404, Ecole Centrale de Lyon, B.P.163 F-69131 Ecully Cedex, France; and †Institut de Recherches sur la Catalyse, CNRS 2, Avenue Albert Einstein, F-69626 Villeubanne Cedex, France

Received September 8, 1993; revised February 25, 1994

Some $VOPO_4$ phases can be involved when the V–P–O catalysts used to oxidize *n*-butane to maleic anhydride are activated. Evidence is given that correct characterization can only be achieved if the catalysts are protected from hydration. Hydration of $VOPO_4$ phases (α_I-, α_{II}-, β-, γ-, δ-) was monitored by Raman spectroscopy. It is shown that, with the exception of β-$VOPO_4$, all $VOPO_4$ phases can be hydrated, with hydration leading to the same $VOPO_4 \cdot 2H_2O$. NH_3 was also intercalated within α_I-$VOPO_4$. These experiments give clues to a unified description of all (with the exception of β-$VOPO_4$) $VOPO_4$ phases as layered arrangements of VO_6 distorted octahedra linked by PO_4 tetrahedra. Proposals are given for the structure of γ- and δ-$VOPO_4$. The proposed structure of δ-$VOPO_4$ allows epitaxy of this peculiar phase onto $(VO)_2P_2O_7$ as well as growth of α_{II}-$VOPO_4$ onto δ-$VOPO_4$.

INTRODUCTION

A number of papers (1–5) have been concerned with the capability of the vanadium phosphate V–P–O system to catalyze *n*-butane oxidation to maleic anhydride. Nonetheless, there is still controversy as to which phases really work during the catalytic process. An entire volume of *Catalysis Today* (6) was recently dedicated to the subject.

Most frequently, catalysts are prepared by thermal activation of the precursor $VOHPO_4 \cdot 0.5H_2O$ in a butane + air flow (7). The activation treatment consists in a gradual increase in temperature from room temperature to 400–450°C, which corresponds to catalytic conditions.

The different authors agree that catalysts are mainly pyrophosphate $(VO)_2P_2O_7$, but as the average oxidation number is usually found to be slightly higher than +4, they think that some phases with vanadium at +5 oxidation number may be involved, particularly during the activation process (8–12).

Review articles on the subject reveal that nomenclature itself (1) differs from one author to another, and that it is sometimes difficult, if even possible, to compare results from different laboratories due to the fact that catalysts are not always sufficiently characterized. In a recent paper (12) we emphasized the characterization of phases of interest in these studies, that is to say, the five different allotropic forms of vanadyl phosphate, α_I-, α_{II}-, β-, γ-, δ-$VOPO_4$, as well as the precursor $VOHPO_4 \cdot 0.5H_2O$, vanadyl pyrophosphate $(VO)_2P_2O_7$, or the dihydrate $VOPO_4, 2H_2O$.

Each of these phases was characterized by its X-ray diffraction pattern, ^{31}P and ^{51}V NMR spectra, and Raman spectrum. We showed that Raman spectroscopy is particularly well suited to studying vanadyl phosphates even in difficult conditions such as in the presence of mixtures or at high temperatures.

Amongst these phases, some are well known, as their structure has been refined: $VOHPO_4 \cdot 0.5H_2O$ (13–14), $(VO)_2P_2O_7$ (15), α_I-, and α_{II}-$VOPO_4$ (16, 17, respectively), and β-$VOPO_4$ (18).

γ- and δ-$VOPO_4$ structures are as yet unknown, even if structural hypotheses have been published (12, 20).

This paper mainly aims to characterize the $VOPO_4$ phases better. In this respect, modification of Raman spectra during hydration is of major importance. We will show that if the dihydrate $VOPO_4 \cdot 2H_2O$ may be observed in used catalysts, this results from careless handling of the samples. Special care must be taken in order to avoid hydration of phases for fear of loss of information regarding the real nature of the catalyst. Hydration will also provide a way to a better understanding of structural relations between these phases and give clues for γ- and δ-$VOPO_4$ structure elucidation.

EXPERIMENTAL

Figure 1 provides an overview of preparation conditions for the pure phases as described elsewhere (12). The phases were characterized by X-ray diffraction, ^{31}P NMR, ^{51}V MAS-NMR, and Raman spectroscopy.

For hydration, all the $VOPO_4$ phases were submitted, at room temperature, to an air flow saturated in water by bubbling through a humidifier. Laser Raman spectroscopy (LRS) examinations were conducted *in situ* in the cell as

[1] To whom correspondence should be addressed. Present address: Département de Chimie, CR4, UFR "Sciences et Techniques," Université de Bretagne Occidentale, B.P. 809, 29285 Brest Cedex, France.

0021-9517/94 $6.00

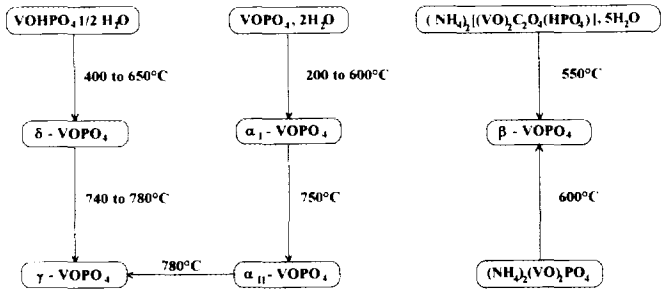

FIG. 1. Overview of preparation conditions of $VOPO_4$ phases (by calcination under air flow).

described elsewhere (12). The hydration process of the $VOPO_4$ phases was followed with continuous registration of the LRS spectra (details are given in Fig. 2's caption).

The α_I-$VOPO_4$ phase was the subject of tentative intercalation of ammonia (NH_3) on a separate glass apparatus. This particular phase was put into contact with pure NH_3 at room temperature and then sealed until the LRS examination. From the beginning to the end of the LRS examination, when the solid was put back into contact with dry air, 10 min elapsed.

Raman spectra were recorded by means of a DILOR OMARS 89 spectrometer equipped with an intensified photo diode array detector (12). The emission line at 514.5 nm of an Ar^+ ion laser (Spectra Physics Model 164) was used for excitation. The power of the beam on the sample was typically around 35 mW. Acquisition time was up to 10 s (typically 3 s) adjusted according to the intensity of Raman scattering. In order to reduce both thermal- and photodegradation of samples, the laser beam was scanned on the sample surface by means of a rotating lens in the way described by Zimmerer and Kiefer (21). The scattered light was collected in the back-scattering geometry.

Thanks to multichannel detection, the 800–1200 cm^{-1} range was accessible in a single shot. As this particular range was sufficient to characterize unambiguously all the phases of interest, it was the only one recorded. Wave number values obtained from experimental spectra were accurate to within about 2 cm^{-1}.

RESULTS AND DISCUSSION

Hydration

With the notable exception of β-$VOPO_4$, which can be considered as insensitive to hydration, all $VOPO_4$ phases undergo a more or less rapid hydration at room temperature.

Figure 2 shows the evolution of Raman spectra of each of the phases α_I-, α_{II}-, γ-, and δ-$VOPO_4$ in the course of hydration. It can be immediately noted that:

(1) In each case the ultimate spectrum was that of the $VOPO_4$, $2H_2O$ phase. This point was confirmed by X-Ray diffraction.

(2) The duration necessary to obtain this particular spectrum depended on the starting phase. While 45 *min* were enough for complete hydration of α_I-$VOPO_4$, it took about 10 h for α_{II}-$VOPO_4$, and about 3 h for both γ- and δ-$VOPO_4$.

(3) At the beginning of α_I-$VOPO_4$ hydration, a new band appeared at about 1010 cm^{-1}, which disappeared after a few minutes. This may have been due to transient formation of the monohydrate $VOPO_4 \cdot H_2O$, a species already reported by several authors (22–24); this particular band has never been observed in other phase hydration.

A more detailed study of spectra changes showed that during hydration of α_I-$VOPO_4$ the experimental spectra resulted from a linear combination of α_I-$VOPO_4$ and $VOPO_4 \cdot 2H_2O$ spectra (with the exception of the 1010

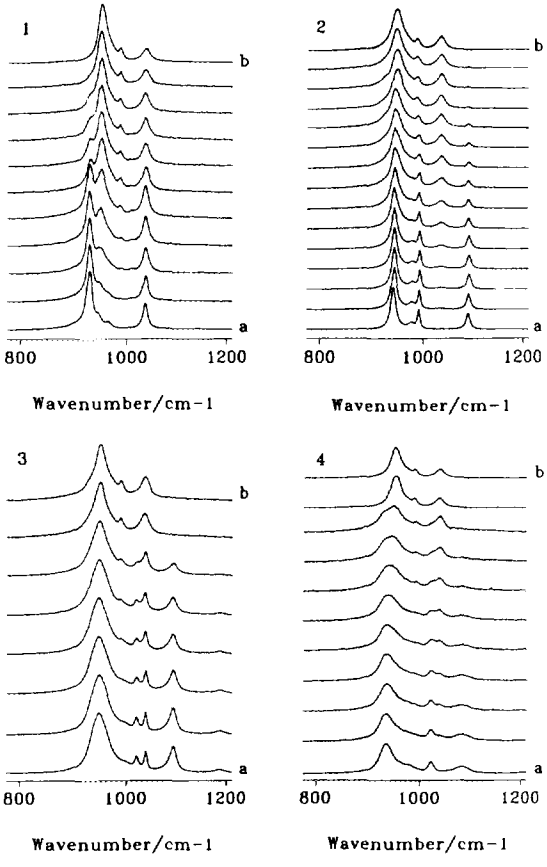

FIG. 2. Evolution of Raman spectra of $VOPO_4$ phases during hydration: (a) before hydration, and (b) after complete hydration. Spectra were acquired in 3 s each with accumulation of 50 to improve signal to noise ratio. Selected spectra, regularly spaced in time, are shown. Complete hydration occurred after 45 *min*, 10 h, 3 h, and 3 h, respectively, for (1) α_I-$VOPO_4$, (2) α_{II}-$VOPO_4$, (3) γ-$VOPO_4$, and (4) δ-$VOPO_4$.

cm^{-1} band). This was not the case for the other phase hydration.

Structural Considerations

These behaviours could easily be understood by comparing the crystalline structures of the phases (when known, i.e., α_I- (16), α_{II}- (17) and β-$VOPO_4$ (18) and $VOPO_4 \cdot 2H_2O$ (19)).

α_I-, α_{II}-, and β-$VOPO_4$ are made up of PO_4 tetrahedra and distorted VO_6 octahedra (a long V···O bond opposed to a short V=O bond and four $V-O_{equatorial}$ bonds). All these phases exhibit alternate long and short bonds giving octahedra chains along the z direction.

In the β-$VOPO_4$ structure each PO_4 tetrahedron links two octahedra belonging to the same octahedra chain (two of the oxygen atoms of the PO_4 are shared with two adjacent octahedra of the same chain), while the other two oxygen atoms are shared with octahedra belonging to different chains (thus, each PO_4 is linked to three octahedra chains). As a result, the β-$VOPO_4$ structure, unlike α-$VOPO_4$, does not exhibit a layered structure.

In the α-$VOPO_4$ structures (both α_I- and α_{II}-), oxygen atoms from every tetrahedron are shared with octahedra belonging to four different chains (22). These phases, as schematically represented in Fig. 3, exhibit a layered structure, the links between adjacent layers being the V···O long bonds.

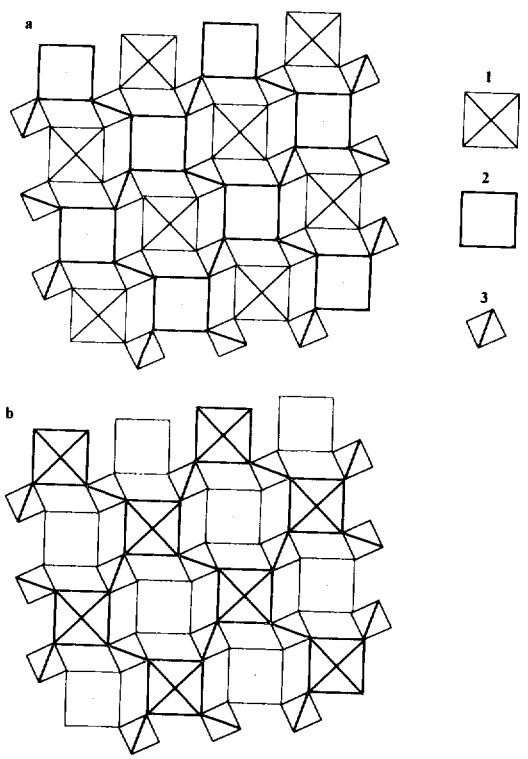

FIG. 3. Schematic representation of α-$VOPO_4$ phase structures: (a) α_I-$VOPO_4$ and (b) α_{II}-$VOPO_4$. (1) and (2) represent VO_6 octahedra, (3) a PO_4 tetrahedron. Heavy lines represent elements on the upper floor (see text), while fine lines are related to the lower floor within the layer. Broken lines indicate that V=O short bonds are directed downwards.

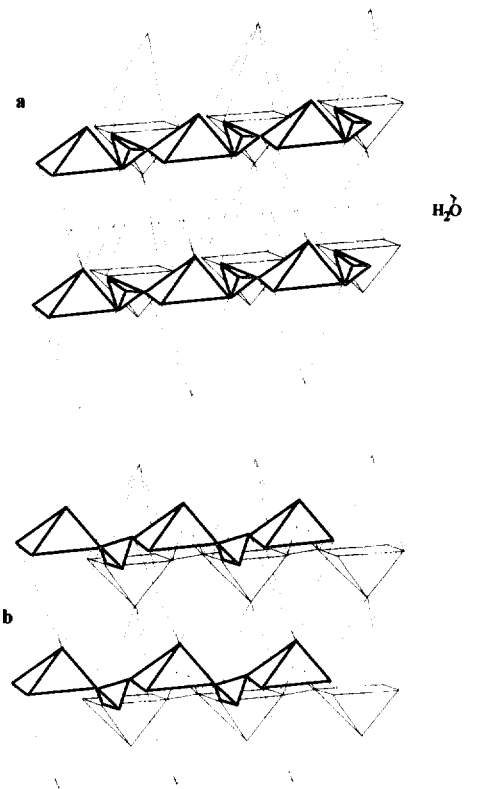

FIG. 4. Interlayer space in (a) α_I-$VOPO_4$ and (b) α_{II}-$VOPO_4$. Obviously, the thickness of layers is greater in the case of α_{II}-$VOPO_4$, while interlayer space is larger and more able to allow water molecule movements in the case of α_I-$VOPO_4$.

The main difference between α_I- and α_{II}-$VOPO_4$ structures is the different positions of vanadium and phosphorus atoms relative to the equatorial plane of the octahedra (22). In α_I-$VOPO_4$, vanadium and phosphorus atoms are on the same side of the equatorial oxygen atom plane, while in the α_{II}-$VOPO_4$ structure they are on opposite sides. It must also be noted that each layer in these phases can be considered to be composed of two sheets, later referred to as the lower and the upper floors. Equatorial oxygen atoms of any VO_6 octahedron belong to the same floor.

In the $VOPO_4 \cdot 2H_2O$ structure, PO_4 tetrahedra—as in α- phases—share their oxygen atoms with octahedra belonging to four different chains. The long V···O bond is replaced by a $V-OH_2$ bond, hydrogen bonds maintaining cohesion between adjacent layers. Vanadium and phosphorus atoms—as in the α_I-$VOPO_4$ phase—are on the same side of the equatorial plane.

Figure 4 shows the interlayer space in α_I- and α_{II}-$VOPO_4$ cases. The space is perfectly open in α_I- and is

large enough to allow water molecule movements, allowing them to interact with vanadium atoms opposite the V=O short bonds without any structural modification within the layers.

It therefore seems logical that during hydration of α_I-$VOPO_4$ we observe mainly a mixture of α_I-$VOPO_4$ and $VOPO_4$, $2H_2O$. In contrast, in the α_{II}-$VOPO_4$ structure the interlayer space is much more congested, short V=O bonds hindering the movement of water molecules, resulting in a much lower hydration rate. Moreover, in this second case, when a water molecule interacts with a vanadium atom, the latter must move inside its octahedral environment from an α_{II}-type position to an α_I- one, to finally give the $VOPO_4 \cdot 2H_2O$ structure. It is thus most probable that in this case hydration occurs through a more intricate process needing more steps than in the α_I-$VOPO_4$ case.

It is worth noting that α_I-$VOPO_4$ hydration, very quick at room temperature, can be avoided by maintaining the sample at a temperature above about 40°C. Temperature effects on α_I-$VOPO_4$ hydration were studied by decreasing the temperature from 140°C to room temperature under wet air flow. It was only below 37°C that the spectrum began to change with the appearance of the characteristic band of $VOPO_4 \cdot 2H_2O$ at 954 cm^{-1}. Moreover, when the temperature of a $VOPO_4$, $2H_2O$ sample was increased from room temperature up to 180°C the spectrum began to change at about 80°C, finally leading to the α_I-$VOPO_4$ spectrum. It has to be pointed out that dehydration of $VOPO_4 \cdot 2H_2O$ samples obtained by hydration of α_I-, α_{II}-, γ-, or δ-$VOPO_4$ always led to α_I-$VOPO_4$. This led to the conclusion that

(1) if $VOPO_4$, $2H_2O$ is observed in used catalysts, it may be the result of careless handling, and

(2) if hydration of $VOPO_4$ phases occurs, there will always be a loss of information as to the previous nature of the compound.

Before discussing the implications of γ- and δ-$VOPO_4$ phase hydration, it is interesting to consider the effect of other intercalated molecules than water.

Such an experiment was done with the α_I-$VOPO_4$ phase only. NH_3 molecules were intercalated between α_I-$VOPO_4$ layers (in a sealed tube). Then subsequent NH_3 desorption—after breaking the tube and contacting a dry atmosphere—was followed by Raman spectroscopy, as previously described. The spectrum (Fig. 5) changed quickly in 10 min due to the evolution of NH_3 molecules, but in contrast to the dehydration process, the final product was not α_I-$VOPO_4$ but a mixture of $VOPO_4$ phases. Unfortunately, complete deconvolution of the corresponding spectra was impossible because these phases were all badly crystallised and the width of Raman bands is known to be crystallinity dependent. However, the final spectrum exhibits sufficient specific features (bands in

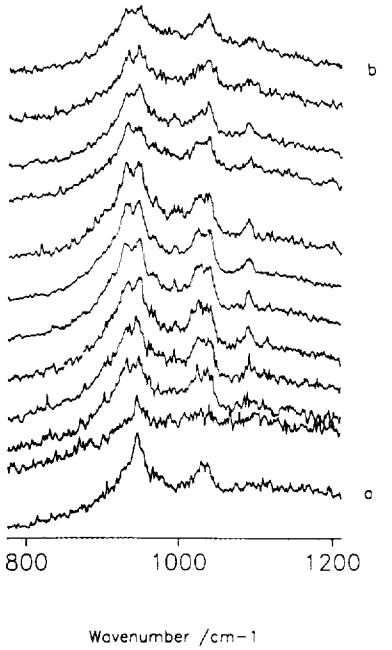

FIG. 5. Evolution of the Raman spectrum of an NH_3-intercalated α_I-$VOPO_4$ during deintercalation. Ten min elapsed between the first and the last spectrum.

characteristic positions, shape of the 1060–1090 cm^{-1} band) to indicate that the final product was a mixture of all $VOPO_4$ phases, with the notable exception of β-$VOPO_4$.

This led us to the hypothesis that α_I-, α_{II}-, γ-, and δ-$VOPO_4$ are built from the same structural units; that is to say, γ- and δ-$VOPO_4$ must possess a layered structure, considering the ease of hydration, and also octahedra chains linked through PO_4 tetrahedra in the way common to α_I- and α_{II}-$VOPO_4$, i.e., each PO_4 tetrahedron sharing its oxygen atoms with VO_6 octahedra from four different chains.

Taking into account arguments from comparison of Raman spectra of the different $VOPO_4$ phases and from the study by Lashier and co-workers (25, 26) of oxidation of vanadyl pyrophosphate $(VO)_2P_2O_7$ to β-$VOPO_4$ by means of $^{18}O_2$, we were able to propose a structural scheme for γ-$VOPO_4$ (12).

Figure 6 shows the arrangement of octahedra and tetrahedra within the layers (6a) and the interlayer space (6b). This space is not so open as in α_I-$VOPO_4$, but not so congested as in α_{II}-$VOPO_4$. In the course of hydration, only one atom of vanadium out of two will have to move from its position in the octahedra to lead to the $VOPO_4 \cdot 2H_2O$ structure in accordance with the respective hydration rates of the phases.

To derive a structural scheme for δ-$VOPO_4$ we used its preparation mode as a guide line. δ-$VOPO_4$ derives from $VOHPO_4 \cdot 0.5H_2O$ by oxydehydration at a temperature comprised between 400 and 580°C (12, 20). We must also

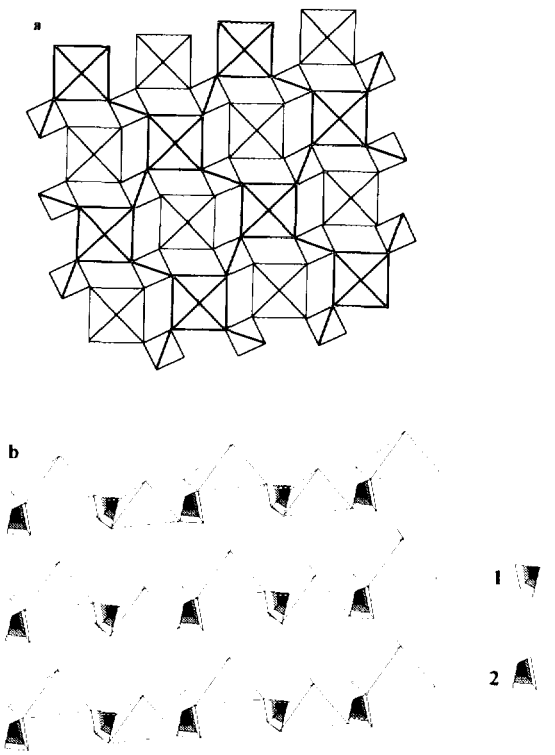

FIG. 6. Idealized structural scheme for γ-$VOPO_4$: (a) projected on a plane parallel to the layers, (b) interlayer space represented in one of the directions given in (a). (1) and (2) represent tetrahedra; black apices indicate their orientation. In order to clearly show interlayer space VO_6 distorted octahedra are represented in a simplified manner.

remember that hydration and NH_3 intercalation experiments led us to the conclusion that δ-$VOPO_4$ must possess a layered structure with the same features (VO_6 octahedra and PO_4 tetrahedra) linked in a similar way as in α_I-, α_{II}-, and γ-$VOPO_4$; i.e., oxygen atoms from every tetrahedron shared with octahedra belonging to four different chains.

Preparation of δ-$VOPO_4$ from $VOHPO_4 \cdot 0.5H_2O$ requires the elimination of water molecules and the oxidation of vanadium from a +4 to a +5 oxidation number. Figure 7 presents an idealized picture of the $VOHPO_4 \cdot 0.5H_2O$ structure (a). Idealizing slightly more, let us suppose that $PO_3(OH)$ can be represented by a true tetrahedron. When the bond between a vanadium atom, V_1, (inside the Oh_1 octahedron) and a water molecule breaks in the presence of an oxidizing atmosphere, the V_1 atom can be oxidized to +5 oxidation number, resulting in a stronger interaction with the equatorial oxygen atoms of its octahedra. The next step may be the oxidation of the V_2 atom (inside the Oh_2 octahedron) to +5 oxidation number with the reconstruction of a "normal" environment by rocking the two nearest tetrahedra, T_1 and T_2. If both rotate in the same direction each of the vanadium atoms will bond with the oxygen of a previous OH and this will probably introduce strong distortion within the layer. If they rotate in opposite directions this will lead to the establishment of new bonds for V_2 (for example) only, V_1 keeping the two oxygen atoms previously shared with V_2. In that case distortions will probably be weaker.

The resulting structure (7b) is a layered one and corresponds to the formula $VOPO_4$. But it is different from the other $VOPO_4$ structures previously described even if it exhibits chains of octahedra with alternate short and long V···O bonds. In $VOHPO_4 \cdot 0.5H_2O$, short V=O bonds of adjacent octahedra are in the *cis* position and the proposed scheme does not change this. A distinctive feature of this structural hypothesis is the appearance of lines of octahedra with their short bonds directed upwards alternating with lines in which they are directed downwards. Ideally, this transformation leads to a structure in which the vanadium atom environments are from the α_I- or the α_{II}- type, one vanadium atom out of two belonging to

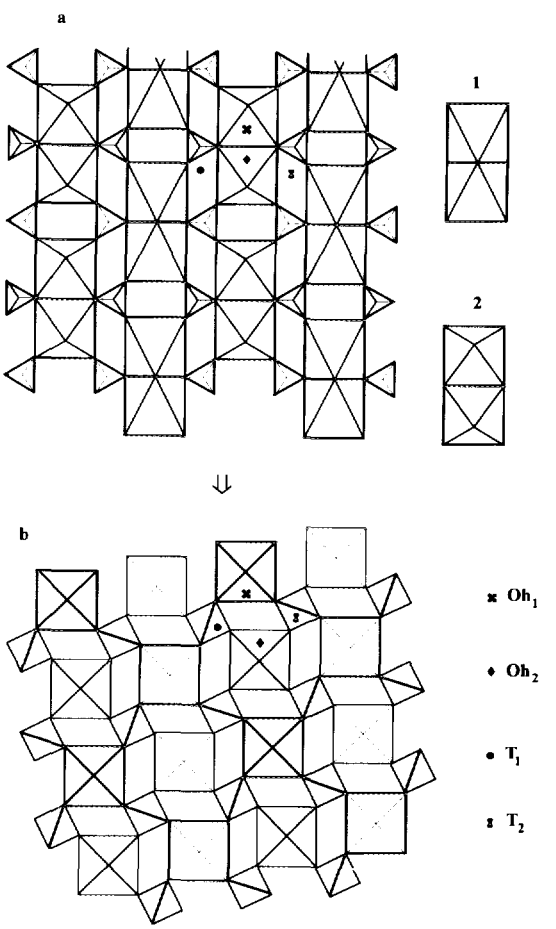

FIG. 7. Proposal for oxydehydration of $VOHPO_4$, $0.5H_2O$ to δ-$VOPO_4$: (a) $VOHPO_4$, $0.5H_2O$ idealized structure, top view. (1) and (2) represent couples of VO_6 octahedra sharing one side, with V=O short bonds directed respectively downwards and upwards. Opposite these bonds are the V–OH_2 bonds. (b) A proposal for the δ-$VOPO_4$ structure projected onto a plane parallel to layers. Oh_1, Oh_2, T_1, and T_2 represent particular octahedra and tetrahedra (see text).

each category. But unlike γ-$VOPO_4$, each α_I- type V^{5+} is not surrounded by α_{II}- type V^{5+} only.

δ-$VOPO_4$ would, then, be made up of the same structural units as the other hydratable $VOPO_4$ phases; that is to say, distorted VO_6 octahedra linked by PO_4 tetrahedra in such a way that each PO_4 tetrahedron shares its oxygen atoms with four VO_6 octahedra belonging to four different chains.

Even if the structure is a layered one, the interlayer space is different from the other $VOPO_4$ layered phases as it exhibits channels separated by bridges in which the layers are as close as in the α_{II}-$VOPO_4$ phase structure. This may lead to distortions giving $V–O_{eq}–P$ angle values comprised between those observed in α_I- and α_{II}-$VOPO_4$. These distortions are most probably less symmetrical than in the case of the γ-$VOPO_4$ structure in which every α_I-type group is surrounded only by α_{II}- types, and conversely. It should be noted that as in γ-$VOPO_4$, hydration requires one vanadium atom out of two to move from its position within its octahedron to actually give the $VOPO_4 \cdot 2H_2O$ structure. It is worth noting that our proposed δ-$VOPO_4$ structural scheme is at variance with the model proposed by E. Bordes with two VO_6 octahedra joined by the edges as in $(VO)_2P_2O_7$ (20). However, it allows the building of a continuous interface between $(VO)_2P_2O_7$ and δ-$VOPO_4$, as well as between δ-$VOPO_4$ and α_{II}-$VOPO_4$. An idealized model for these interfaces is shown on Fig. 8.

This point must also be related to the observation by *in situ* Raman spectroscopy of δ- and α_{II}-$VOPO_4$ in a catalyst obtained by activation of the precursor $VOHPO_4 \cdot 0.5H_2O$ (11), and the partial transformation of δ-$VOPO_4$ to α_{II}-$VOPO_4$ under conditions of butane-selective oxidation to maleic anhydride, i.e., butane + air flow at a temperature around 420°C (12).

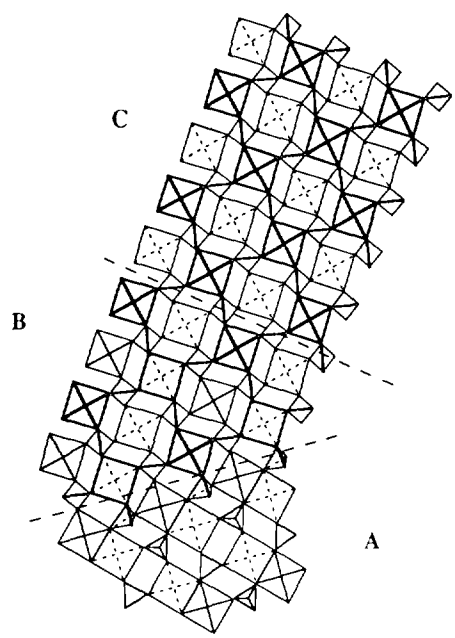

FIG. 8. Structure of interfaces between $(VO)_2P_2O_7$ (A) and δ-$VOPO_4$ (B), and between δ-$VOPO_4$ (B) and α_{II}-$VOPO_4$ (C).

CONCLUSION

In this paper we demonstrated that four allotropic forms of $VOPO_4$ are easily hydrated to give $VOPO_4 \cdot 2H_2O$, resulting in a loss of information as to the previous nature of the V(+5) phase when hydration occurs.

We were also able to state that all $VOPO_4$ phases, with the exception of β-$VOPO_4$ may be represented by a general scheme. All these phases must possess:

(1) chains of VO_6 octahedra with alternate long V···O and short V=O bonds;

(2) PO_4 tetrahedra, each linked to four octahedra belonging to four different chains; and

(3) layered structures in which two distinct levels of equatorial oxygen atoms (bottom floor and upper floor) can be observed.

Differences between these phases are mainly due either to different arrangements of octahedra within the layers or relative to tetrahedra.

In α_I-$VOPO_4$, V=O short bonds are directed to the interior of the layer (the oxygen atoms of the V=O short bonds are between the bottom and the upper floors).

In α_{II}-$VOPO_4$, each V=O short bond is directed outwards (the oxygen atoms of the V=O short bonds are below the bottom floor or above the upper floor).

In γ-$VOPO_4$, every V=O short bond is presumed to be directed in one direction (say upwards) regardless of belonging to the bottom or the upper floor.

δ-$VOPO_4$ is presumed to exhibit lines of adjacent octahedra with their V=O short bonds directed upwards alternating with lines in which they are directed downwards, regardless of belonging to the bottom or the upper floor.

We also show that, on this basis, continuous coherent interfaces may be built between $(VO)_2P_2O_7$ and δ-$VOPO_4$ and between δ- and α_{II}-$VOPO_4$, which may explain the occurrence and transformations of the last two phases in the working catalyst during transformation of *n*-butane to maleic anhydride.

Of course, it should be remembered that this scheme is an idealized one.

REFERENCES

1. Hodnett, B. K., *Catal. Today* **1,** 477 (1987).
2. Centi, G., Trifiro, F., Ebner, J. R., and Franchetti, J. M., *Chem. Rev.* **88,** 55 (1988).
3. Bordes, E., *Catal. Today* **1,** 499 (1987).
4. Shimoda, T., Okuhara, T., and Misono, M., *Bull. Chem. Soc. Jpn.* **58,** 2163 (1985).
5. Moser, T. P., and Schrader, G. L., *J. Catal.* **92,** 216 (1985).

6. *Catal. Today*, **16,** 1–153 (1993). (the entire volume)
7. Hutchings, G. J., *Appl. Catal.* **72,** 1 (1991).
8. Centi, G., Fornasari, G., and Trifiro, F., *J. Catal.* **89,** 44 (1984).
9. Contractor, R. M., Bergna, H. E., Horowitz, H. S., Blackstone, C. M., Malone, B., Torardi, C. C., Griffiths, B., Chowdhury, U., and Sleight, A. W., *Catal. Today* **1,** 49 (1987).
10. Contractor, R. M., and Sleight, A. W., *Catal. Today* **3,** 175 (1988).
11. Volta, J. C., Bere, K., Zhang, Y. J., and Olier, R., *in* "Catalytic Selective Oxidation" (S. T. Oyama and J. W. Hightower, Eds.), ACS Symposium Series, Vol. 523, p. 217. Amer. Chem. Soc., Washington, D.C., 1993.
12. Benabdelouahab, F., Olier, R., Guilhaume, N., Lefebvre, F., and Volta, J. C., *J. Catal.* **134,** 151 (1992).
13. Leonowicz, M. E., Johnson, J. W., Brody, J. F., Shannon, M. F., and Newsam, J. M., *J. Solid State Chem.* **56,** 370 (1985).
14. Torardi, C. C., and Calabrese, J. C., *Inorg. Chem.* **23,** 1308 (1984).
15. Linde, S. A., Gorbunova, Yu. E., Lavrov, A. V., and Kuznetsov, V. G., *Dokl. Akad. Nauk SSSR* **245,** 584 (1979).
16. Bordes, E., Courtine, P., and Pannetier, G., *Ann. Chim. Paris* **8,** 105 (1973).
17. Jordan, B., and Calvo, C., *Can. J. Chem.* **51,** 2621 (1973).
18. Gopal, R., and Calvo, C., *J. Solid State Chem.* **5,** 432 (1972).
19. Tietze, H. R., *Aust. J. Chem.* **34,** 2035 (1981).
20. Bordes, E., Johnson, J. W., Raminosona, A., and Courtine, P., *Mater. Sci. Monogr.* **28B,** 887 (1985).
21. Zimmerer, N., and Kiefer, W., *Appl. Spectrosc.* **28,** 279 (1974).
22. Tachez, M., Theobald, F., and Bordes, E., *J. Solid State Chem.* **40,** 280 (1981).
23. Tachez, M., Theobald, F., Bernard, J., and Hewat, A. W., *Rev. Chim. Miner.* **19,** 291 (1982).
24. R'kha, C., Vandenborre, M. T., Livage, J., Prost, R., and Huard, E., *J. Solid State Chem.* **63,** 202 (1986).
25. Lashier, M. E., Moser, T. P., and Schrader, G. L., *in* "Surface Science and Catalysis" (G. Centi, and F. Trifiro, Eds.), Vol. 55, p. 573. Elsevier, Amsterdam, 1990.
26. Lashier, M. E., and Schrader, G. L., *J. Catal.* **128,** 113 (1991).